

# Improving the intercalibration of $\sigma^0$ values for the Jason-1 and Jason-2 altimeters

Graham D. Quartly

National Oceanography Centre, Southampton

email: gdq@noc.soton.ac.uk

(Sub. to IEEE Geoscience & Remote Sensing Letters 14th Feb. 2009; in final form 6th April 2009)

## Abstract

The normalized backscatter from a radar altimeter,  $\sigma^0$ , is a measure of the surface roughness at scales of a few radar wavelengths; over the ocean this is used to infer wind speed. Long-term studies of wind speed rely on consistent measurements within an altimetric mission and good intercalibration between missions. For the Jason-1 and Jason-2 altimeters the derivation of  $\sigma^0$  from the full waveform data is known to be sensitive to the recovered value for  $\psi^2$ , a term encompassing both mispointing and inhomogeneities within the altimetric footprint. The six months of data from the Jason-1/2 tandem mission reveal that different  $\sigma^0$  corrections are needed for these two causes of non-zero  $\psi^2$  values. With these corrections implemented, the r.m.s. difference of K<sub>u</sub>-band  $\sigma^0$  values for Jason-1 and Jason-2 drops from 0.15 dB to 0.05 dB, with the bias between the two showing a clear trend with wind speed; Jason-1 being 0.04 dB greater in high winds but 0.19 dB greater in low winds. No clear change in offset is noted during the 6 months of overlapping data. Implementation of this correction will improve consistency of Jason-1  $\sigma^0$  values and may impact on orbit-fitting procedures.

**Keywords** — altimeter, sigma0, Jason-1, Jason-2, cal/val, tandem mission

## 1. Introduction

Spaceborne radar altimeters emit pulses of radar waves and record their reflection from the surface of the Earth. A number of such echoes are added together to give a mean waveform (Fig. 1) and various geophysical parameters obtained by fitting a model to the data [1]. For the Jason-1 and Jason-2 instruments considered here, 90 Ku-band (13.575 GHz) pulses are summed every 0.0508 s and a 4-parameter model fitted [2]. Originally for Jason-1 (launched Dec. 2001) only 3 geophysical parameters were fitted: range (time delay to middle of leading edge), significant wave height (SWH, slope of leading edge) and  $\sigma^0$  (amplitude). That fitted model is based on the assumption that the instrument is pointing at nadir; however for Jason-1 the mispointing was severe enough (more than one quarter of the beamwidth) that the slope of the trailing edge of the waveform departed from the value expected for a nadir-pointing instrument. Thus the currently used 4-parameter model [2] also fits  $\psi^2$ , the change in trailing edge slope. This term encompasses the effect of genuine mispointing (which should correspond to  $\psi^2 > 0$  and time scales of more than 500 s) and inhomogeneities in surface scattering or atmospheric attenuation within the altimetric footprint (whose effect may be positive or negative and should be uncorrelated at times greater than 10s i.e. the time needed to transverse one strong rain cell, surface slick or wind front).

However the joint estimation of  $\sigma^0$  and  $\psi^2$  is ill-conditioned as was shown theoretically by Challenor and Srokosz [3], and demonstrated for Jason-2 data by Quartly [4]. That work concentrated on the short scale (20 Hz) changes in  $\psi^2$  and found that the corresponding changes in  $\sigma^0$  are linearly related by a coefficient, which varies only slightly according to the on-board acquisition tracker [4]. Comparisons between Jason-1 and Jason-2 data show that this adjustment is not valid when long-term mispointing occurs for Jason-1. A hint of the importance of allowing for  $\psi^2$  had been shown in an earlier comparison of TOPEX and Jason-1 data during that tandem mission [5]. In section 2, I detail the data used here, and discuss the characteristics of the mispointing values for both satellites. Section 3 introduces the improved correction model, treating short- and long-scale variations in  $\psi^2$  separately, and discusses the implications. [ In this paper all analysis is of K<sub>u</sub>-band data unless otherwise explicitly stated; the effects at the altimeters' second frequency (C-band, 5.3 GHz) are much reduced [4] owing to its greater beamwidth. ]

## 2. Data selection and filtering

Jason-2 was launched on 20th June 2008 and placed in an orbit 55 seconds behind Jason-1. The two satellites thus provided near-simultaneous observations of the same points of the ocean until the end of the tandem phase on 26th January 2009. The data from the interim geophysical data records (IGDR) are readily available for both Jason-1 and Jason-2, and the quality of their  $\sigma^0$  data matches that of "final" products. Those data provide a great source for intercalibration of Jason-1 and Jason-2. Usually such exercises are accomplished using the 1 Hz data (directly available in the data stream as averages of the 20 Hz data), with linear interpolation to collocate the two sets of data.

However, as  $\psi^2$  has such marked short-term variations, here I regroup the Jason-2 20 Hz data to calculate 1 Hz averages of  $\psi^2$  and  $\sigma^0$  closely matching the Jason-1 locations. (The Jason-1 data are not regrouped as they do not contain 20 Hz values for  $\psi^2$ .) After editing to remove any possible contamination by land, rain or sea-ice, I have for each cycle of data, typically  $3 \times 10^5$  match-ups of Jason-1 and Jason-2 data coinciding to within 1.1 km. The examples shown in this paper correspond to Jason-2 cycle 012 (Jason-1 cycle 251), but the final analysis has been performed using all the data from the tandem mission together.

In an earlier paper [4], I developed a simple means of improving the quality of Jason-2  $\sigma^0$  data by calculating an adjusted value,  $\sigma_{\text{adj}}^0$  that overcomes the errors induced by overfitting the waveform using the 4-parameter model, viz:

$$\sigma_{\text{adj}}^0 = \sigma^0 - 11.34 \psi^2 \quad (1)$$

This model was very effective at removing small-scale variability in  $\sigma^0$  and improving the efficacy of rain-flagging [4]. However for Jason-1 data this correction only appears to be appropriate when the actual mispointing (assumed to equal the long-term mean of  $\psi^2$ ) is negligible. For Jason-1, platform mispointing has been a problem, hence the introduction of the 4-parameter model [2]. The characteristics of  $\psi^2$  for Jason-1 and Jason-2 are shown in Fig. 2. The top panel, covering a short segment of collocated  $\psi^2$  data, shows how the short-scale variations match up (indicating that the surface inhomogeneities that cause them change little in 55 s) despite the long-term offset of the Jason-1 values (due to genuine mispointing). The second panel shows 30-s averages,  $\psi^2_{30s}$ , indicating the quasi-periodic nature of the mispointing for Jason-1. There is a gradual increase as the platform veers from nadir, followed by an abrupt return (over 50-100s) to near zero, presumably due to a response by the reaction wheels. For the section of data illustrated, ascending passes are spanning the Pacific and  $\psi^2_{30s}$  reaches 0.13-0.15 deg<sup>2</sup> before returning to zero near 50°N; the descending passes over the Indian Ocean reach 0.03 deg<sup>2</sup>, with zeroing near 36-40°S. Figure 2c shows the spectra of  $\psi^2$  variations for both altimeters plus their coherence; the latter shows pronounced co-variation for periods between 3 and 70 seconds (or equivalently spatial scales between 17 and 400 km). For this work, I define a long-term mean,  $\psi^2_{lo}$ , as the result of a 140-point (800 km) running mean of  $\psi^2$  over the ocean, once the extreme spikes have been removed. Visual inspection shows that this two-stage process (despiking and smoothing) fits the long-term behaviour well. (Data over rivers and lakes, and also those near the reaction wheel responses are not included in the later analysis, because of the difficulty in defining an appropriate mean.) The characteristics of these filtered data are shown in Fig. 2d; the values for Jason-1 vary between 0 and more than 0.10 (as shown in Fig. 2b), whereas  $\psi^2_{lo}$  for Jason-2 is usually about 0.01. Indeed a mean value of 0.012 is found for each Jason-2 cycle (Fig. 2e); this is an estimate from initial waveform fitting, and later versions of the data may show a slightly lower value, after modification of the waveform model.

### 3. Developing an improved model

#### 3.1 Sigma0 comparisons

The mean  $\sigma^0$  value for Jason-1,  $\bar{\sigma}^0$ , is 13.7 dB. Analysis of the  $\sigma^0$  discrepancy,  $\sigma^0_{J2-J1}$  (Fig. 3a) shows that Jason-2 gives lower values than Jason-1, and by an amount that increases in magnitude with  $\sigma^0$ . The best fit line is given by:

$$\sigma^0_{J2-J1} = c + d (\sigma^0_{J1} - \bar{\sigma}^0) \quad (2)$$

with fitted values  $c = -0.09$ ,  $d = -0.034$  leading to an r.m.s. scatter about the line of 0.150 dB. The correction for mispointing advocated by Quartly [4] can significantly improve the quality of this match-up, provided there is no long-term mispointing. To demonstrate this I select data for which both Jason-1 and Jason-2 have  $\psi^2_{lo}$  values close to 0.01. For this selected subset of near-constant  $\psi^2_{lo}$ , the scatter is slightly less (0.139 dB) but is greatly reduced (to 0.060 dB) on applying Eq. 1 to both the Jason-1 and Jason-2 data (Fig. 3b). However, if this correction is applied to all the data, it is not so effective (Fig. 3c). The solution is to modify Eq. 1 to allow for different adjustment factors for the short- and long-term variations in  $\psi^2$ , viz:

$$\sigma_{\text{adj}}^0 = \sigma^0 - \alpha (\psi^2 - \psi^2_{lo}) - \beta \psi^2_{lo} \quad (3)$$

Assuming the  $\sigma^0$  discrepancy will still have a linear form (representing small errors in the knowledge of instrument attenuation and scaling), one can define the error,  $e$ , in the explained match-up by substituting Eq. 3 into Eq. 2:

$$e = \sigma_{\text{adj}, J2}^0 - \sigma_{\text{adj}, J1}^0 - (c + d (\sigma_{\text{adj}, J1}^0 - \bar{\sigma}^0)) \quad (4a)$$

$$= \sigma_{J2}^0 - \alpha_{J2} (\psi_{J2}^2 - \psi_{lo, J2}^2) - \beta_{J2} \psi_{lo, J2}^2 - (1+d)\sigma_{J1}^0 \\ + (1+d) \alpha_{J1} (\psi_{J1}^2 - \psi_{lo, J1}^2) + (1+d) \beta_{J1} \psi_{lo, J1}^2 - (c - d) \bar{\sigma}^0 \quad (4b)$$

where J1 or J2 in the subscript indicates the relevant altimeter. For this cycle of data, least squares solution gives  $\alpha_{J1} = 11.23$ ,  $\alpha_{J2} = 11.37$ ,  $\beta_{J1} = -1.48$ ,  $\beta_{J2} = 2.75$ ,  $c = -0.14$ ,  $d = -0.030$ , with the resultant r.m.s. value,  $e$ , being 0.047 dB. The resultant tight relationship between  $\sigma_{\text{adj}, J1}^0$  and  $\sigma_{\text{adj}, J2}^0$  is seen in Fig. 3d, where the scatter is low even at high  $\sigma^0$  values.

### 3.2 Implications and interpretation

It is apparent from the preceding analysis that greatest consistency between Jason-1 and Jason-2  $\sigma^0$  values is achieved by a two-term correction for derived mispointing. The first term,  $\alpha$ , is due to overfitting of the waveform as determined from 20 Hz analysis of Jason-2 data [4], and should be applied to the high-frequency variations in  $\psi^2$  which are due to inhomogeneities within the altimetric footprint. The second term,  $\beta$ , is a correction for genuine mispointing, which varies on much larger timescales. It is the latter term that affects climatologies of wind speed. This can be illustrated by comparing Jason-1 data for descending and ascending passes, since  $\psi^2_{lo,J1}$  has strong regional variations (as hinted at by Fig. 2b). For cycle 251 I determine climatologies of  $\sigma^0_{J1}$  and  $\psi^2_{lo,J1}$  on a  $2.5^\circ \times 2.5^\circ$  grid (limited to  $55^\circ S$  to  $55^\circ N$  to avoid sea-ice), treating the descending and ascending passes separately. The climatologies of  $\psi^2_{lo,J1}$  (not shown) display strong spatial coherence, with the difference between them ranging from  $-0.12$  to  $0.04$  deg $^2$ . Although both the  $\sigma^0_{J1}$  climatologies reflect the known mean pattern of wind speed, their difference is highly variable due to storms and fronts moving during the interval between descending and ascending passes. However, a simple regression of the changes in  $\sigma^0_{J1}$  and  $\psi^2_{lo,J1}$  (Fig. 4) does suggest a dependency ( $-1.37$  dB deg $^{-2}$ ), although the 95% confidence interval does also include zero. Thus a consistent estimate of  $\beta_{J1}$  can be determined using Jason-1 data alone; however, the errors for such a method are much greater on account of the temporal variations in  $\sigma^0$  between ascending and descending passes.

The interpretation of  $\beta_{J1}$  is problematic. It differs in magnitude and sign from  $\alpha_{J1}$  yet there is no direct link between  $\psi^2$  and  $\sigma^0$  other than in the waveform-fitting process. The value of  $\alpha_{J1}$  of  $\sim 11$  is consistent with a simple Gaussian antenna pattern for that size antenna; the very different value for  $\beta_{J1}$  (i.e. the net relationship between actual instrument mispointing and recorded  $\sigma^0$ ) suggests either a more complicated effect causing mispointing to increase the signal returned, or that there is automatic compensation in the signal processing. Although, for TOPEX there was an explicit  $\sigma^0$  correction based on mispointing and wave height [6], such a correction is not present for Jason-1.

### 3.3 Stability of solution

All the cycles of the tandem phase have been separately processed to provide first the match-up characteristics of the original unadjusted data, and second the coefficients that minimize the error term in Eq. 4. These independent evaluations are shown in Fig. 5. Similar values were achieved when  $\psi^2_{lo}$  was produced using a 70-point, rather than 140-point, smoother, showing that the regression analysis is not overly sensitive to the definition of  $\psi^2_{lo}$ . Ideally the platform-based value,  $\psi^2_{pf}$ , which needs no smoothing, would provide the required measure; however those values are not available on the IGDRs, and will require further analysis to compare their scaling with  $\psi^2_{lo}$ . In general the results show good consistency between different cycles of data.

The values for  $\alpha_{J2}$  obtained by this method (Fig. 5d; mean=11.29) match that obtained by the 20 Hz intra-footprint study of Jason-2 data alone (11.34, see [4]). The value for Jason-1 is slightly less (mean=11.08), with the difference possibly being attributable to a slightly different mean waveform shape, plus the effect of incomplete data on the fitting process (in the second half of the waveform, Jason-1 data were averaged in groups of five, see Fig. 1, whereas that was not done for Jason-2). There is also a strong correlation between the derived values for Jason-1 and Jason-2, because the high-frequency variations in  $\psi^2_{J1}$  and  $\psi^2_{J2}$  are highly correlated (see Figs. 2a,c).

However, the low frequency adjustment,  $\beta$ , is also important in improving the match-up of  $\sigma^0$  data (compare Figs. 3c & d), with the coefficient for Jason-1 (Fig. 5e) having a mean of -1.26 (std. dev. of cycle estimates is 0.40). The values derived for Jason-2 are highly variable and differ from  $\beta_{J1}$ . However, the estimates of  $\beta_{J2}$  are not robust, because  $\psi^2_{lo,J2}$  has much less dynamic range than  $\psi^2_{lo,J1}$  (see Fig. 2d) and these weak  $\psi^2_{lo,J2}$  variations may potentially map on to latitudinal variations in  $\sigma^0_{J1}$  (one of the other regression variables). Thus, whilst the pointing of Jason-2 remains stable, the  $\beta_{J2}$  term may be set to zero and the contribution due to the mean value of  $\psi^2_{lo,J2}$  folded into the offset term. Table 1 shows the results for an inversion of all 6 months of data, with  $\beta_{J2}$  set to zero. This details the most appropriate coefficients for correcting both altimeters for mispointing and for adjusting Jason-2 values to match Jason-1.

The contribution of these corrections to the match-up of  $\sigma^0$  values from Jason-1 and Jason-2 is considerable, with ~90% of the variability explained (Fig. 5f) and the r.m.s. match-up errors reduced to a third (Fig. 5c). These major changes have only a slight effect on the coefficients c and d required for a bulk correction of Jason-2 data to a Jason-1 norm (Figs. 5a,b). The change in offset is due to the effect of the  $\beta$  term and the long-term mean of  $\psi^2$ . There is also a change in the slope by about 0.004 i.e. 0.04 dB variation in offset over the range 8 to 18 dB. This is due to a geographical correlation: generally the regions of high  $\sigma^0$  are the low latitudes, which have higher  $\psi^2$  values than the higher latitudes.

Whilst Quartly [4] pointed out that correction for the  $\alpha$  term was important for rain studies [7,8] and other dual-frequency applications, adjustment for the  $\beta$  term is important for consistent long-term climatologies of wind speed, and will also make data from Jason-1 ascending and descending tracks more consistent (Fig. 4). It also has implications for the sea state bias (SSB) correction [9]. The functions for converting  $\sigma^0$  to wind speed, and then wind speed to SSB are non-linear, but guidance values are that a mispointing,  $\psi^2_{lo}$  of  $0.10 \text{ deg}^2$  will cause a change in wind speed of up to  $0.5 \text{ ms}^{-1}$  and in SSB of order  $0.3 \text{ cm}$ . For a given cycle of data, only a small proportion will have  $\psi^2_{lo}$  values exceeding  $0.10 \text{ deg}^2$ ; however, because  $\psi^2_{lo}$  has strong regional patterns, the biased measures of wind speed and SSB will be clustered together. This is not only important in terms of a direct effect on sea level studies, but also has implications for crossover adjustment of altimeter orbits because of the pronounced regional differences in  $\psi^2_{lo}$  between ascending and descending passes.

## 4. Conclusions

The Jason-1/2 tandem mission offers an unprecedented opportunity to understand the intricacies of accurate  $\sigma^0$  retrieval on account of the near-simultaneous observations by two similar altimeters. The  $\psi^2$  information, coming from the retracker has two very different origins: the high-frequency component relates to surface or atmospheric inhomogeneities within the altimetric footprint and is highly correlated between the two instruments (Fig. 2c), whereas the low-frequency part is due to mispointing, which is generally only a problem for Jason-1 (Fig. 2e).

A simple comparison of  $\sigma^0_{Ku}$  from the Jason-1 and Jason-2 instruments shows the latter to read lower by  $0.09 \text{ dB}$ , with a significant trend in  $\sigma^0$  (Eq. 2) and an r.m.s. scatter of  $0.15 \text{ dB}$ . (Adjustments in ground processing since the tandem phase mean that more recently-processed Jason-2 data will be a further  $0.05 \text{ dB}$  below the Jason-1 values.) Taking into account the two-term  $\psi^2$  correction introduced in Eq. 3 reduces the scatter to  $0.05 \text{ dB}$  and also reduces the magnitude of the trend slightly. (The derived offset,  $c$ , changes from  $-0.09 \text{ dB}$  to  $-0.11 \text{ dB}$  principally to compensate for  $\beta_{J1}$  times the mean of  $\psi^2_{lo,J1}$ .) The derived coefficients are robust for the duration of the tandem mission (Fig. 5) and consistent with earlier work. As the mispointing and the regions affected change from cycle to cycle, these corrections should be applied in the development of consistent data for climatological studies. There are also implications for sea surface height data, due to the use of  $\sigma^0$  in SSB corrections, and that regional biases will feed into orbit determination via crossover techniques. The provision of actual measurements of platform mispointing,  $\psi^2_{pf}$ , would probably simplify the implementation of code to determine the high- and low-frequency components of  $\psi^2$  and correct for their effect on  $\sigma^0$ .

It is somewhat amusing that this tandem phase, intended for calibration of Jason-2, may yield the greatest improvements in our understanding of Jason-1  $\sigma^0$  data.

## Acknowledgements

The author is grateful to Remko Scharroo and Pierre Thibaut for helpful discussions both before this paper was started and as it was written. Jason-2 IGDR data were obtained from the CLS FTP server, under the OSTST-approved project 'TRIDENT II'.

## References

- [1] G.S. Brown, The average impulse response of a rough surface and its applications, *IEEE J. Oceanic Eng.*, vol. 2, 67–74, 1977.
- [2] L. Amarouche, P. Thibaut, O.-Z. Zanife, J.P. Dumont, P. Vincent, and N. Steunou, Improving the Jason-1 ground tracking to better account for attitude effects, *Marine Geodesy*, vol. 27 (1-2), 171-197, 2004.
- [3] P.G. Challenor, and M.A. Srokosz, The extraction of geophysical parameters from radar altimeter returns from a non-linear sea surface, in *Mathematics in Remote Sensing* (ed. S.R. Brooks), Clarendon Press, 1989.
- [4] G.D. Quartly, Optimizing  $\sigma^0$  information from the Jason-2 altimeter (to appear in *IEEE Geosci & Remote Sensing Lett.*), doi: 10.1109/LGRS.2009.2013973, 2009.
- [5] G.D. Quartly, Sea state and rain: A second take on dual-frequency altimetry, *Marine Geodesy*, vol. 27 (1-2), 133-152. & 27 (3-4), 789-795, 2004.
- [6] G.S. Hayne, D.W. Hancock, C.L. Purdy, and P.S. Callahan, The corrections for significant wave height and attitude effects in the TOPEX radar altimeter, *J. Geophys. Res.*, vol. 99, 24 941-24 955, 1994.
- [7] G.D. Quartly, T.H. Guymer, and M.A. Srokosz, The effects of rain on Topex radar altimeter data, *J. Atmos. Oceanic Tech.* vol. 13, 1209-1229, 1996.
- [8] G.D. Quartly, M.A. Srokosz and T.H. Guymer, Global precipitation statistics from dual-frequency TOPEX altimetry, *J. Geophys. Res.* vol. 104 (D24), 31489-31516, 1999.
- [9] P. Gaspar P., F. Ogor, P.-Y. Le Traon, and O. Z. Zanife, Estimating the sea state bias of the TOPEX and POSEIDON altimeters from crossover differences. *J. Geophys. Res.*, vol. 99, 24981-24994, 1994.

Coefficient	Ku	C
$\alpha_{J1}$ (dB deg $^{-2}$ )	11.14	1.77
$\alpha_{J2}$ (dB deg $^{-2}$ )	11.30	1.72
$\beta_{J1}$ (dB deg $^{-2}$ )	-1.40	-0.65
Offset, c (dB)	-0.11	-0.18
Slope, d	-0.024	-0.010
r.m.s. matchup (dB)	0.049	0.057
% explained	89.0	19.0

Table 1 : Optimal coefficients to improve match-up of Jason 1 and Jason-2 near-simultaneous  $\sigma^0$  values (as in Eq. 4b, with  $\bar{\sigma}^0 = 13.7$  dB (Ku) or 15.4 dB (C) and  $\beta_{J2}$  set to zero)

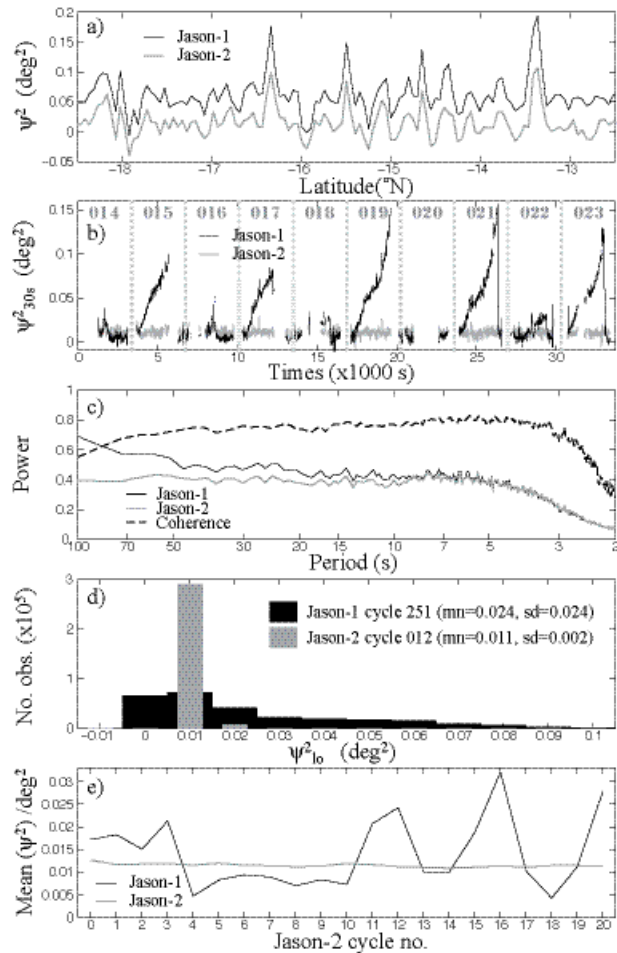


Fig. 2 : Characteristics of  $\psi^2$  for Jason-1 cycle 251 and Jason-2 cycle 012. a) Short segment from pass 015. b) Smoothed despiked  $\psi^2$  data from passes 014 to 023. c) Average spectra of  $\psi^2$ , and coherence of Jason-1 and Jason-2 variations (based on 512-pt continuous segments). d) Histogram of filtered values,  $\psi^2_{lo}$ . e) Mean value of  $\psi^2$  for each Jason-1 cycle of data.

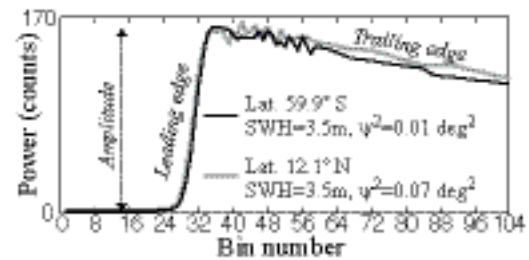


Fig. 1 : Examples of Jason-1 1-sec average waveforms from cycle 251, pass 015.

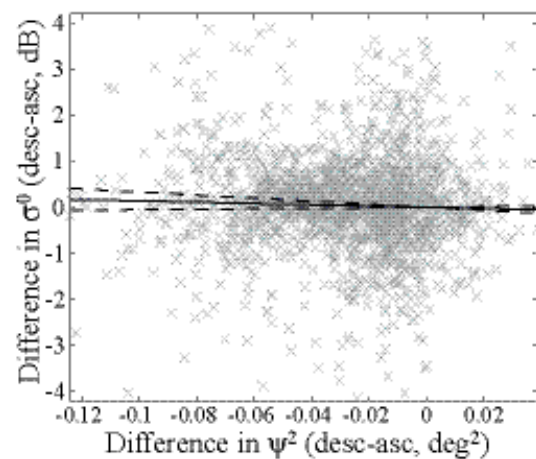


Fig. 4 : Comparison of Jason-1 gridded products (descending and ascending passes for cycle 251 separately averaged to a  $2.5^\circ \times 2.5^\circ$  grid), showing change in  $\sigma^0$  as a function of change in  $\psi^2_{lo}$ . Solid line shows least squares fit (slope =  $-1.37$  dB deg $^{-2}$ ), with dashed lines showing 95% confidence interval ( $[-3.28, 0.55]$  dB deg $^{-2}$ ).

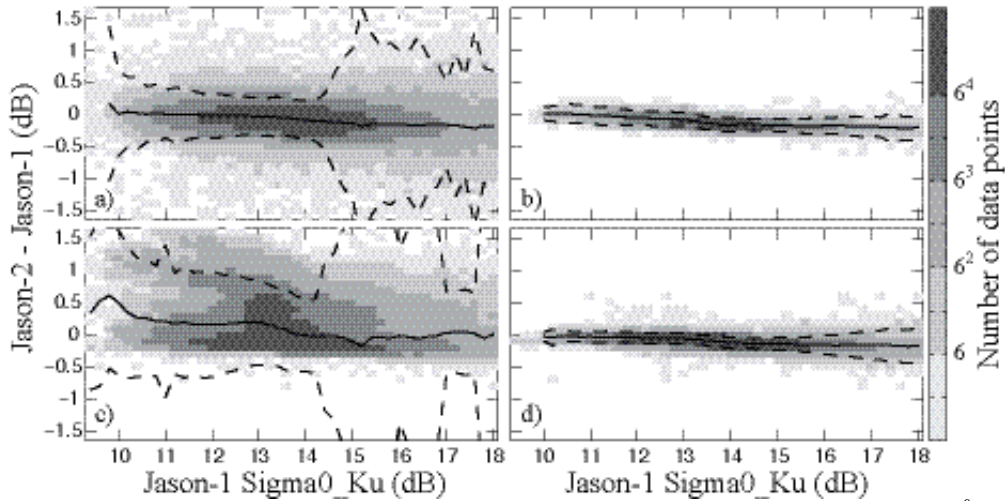


Fig. 3 :  $\sigma^0$  discrepancy (Jason-2 cycle 012 relative to Jason-1 cycle 251) as function of Jason-1  $\sigma^0$  for various stages of processing. Shading shows 2-D histograms, with superimposed solid lines giving mean and dashed lines  $\pm 2$  std. dev. in each 0.2 dB bin. a) Original i.e. all data, with no correction. b) Subset with  $\psi_{lo}^2=0.01$ , corrected according to Eq. 1. c) All data corrected according to Eq. 1. d) All data corrected according to Eq. 4b.

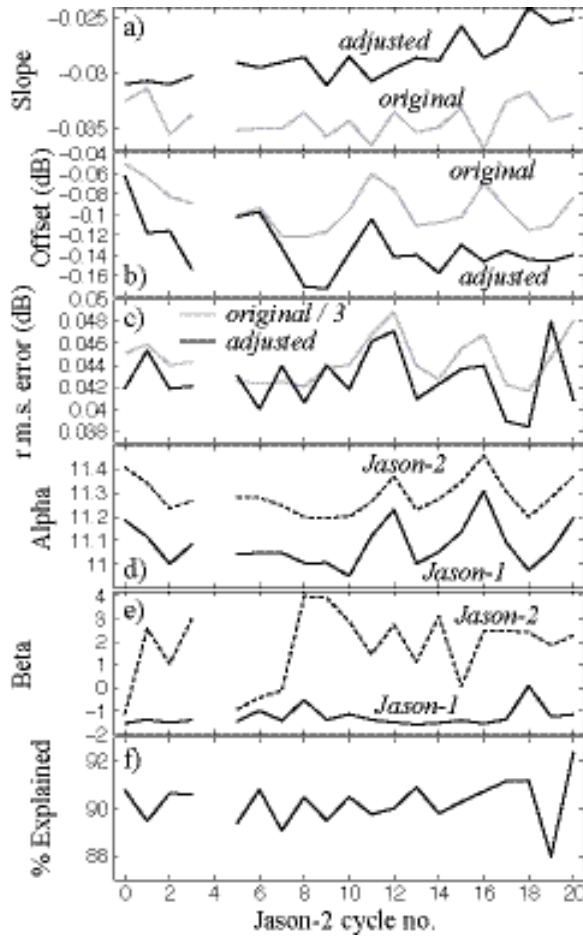


Fig. 5 : Time series of fitting parameters for each cycle of tandem mission. (Jason-1 was not operating for most of Jason-2 cycle 004 hence no values are shown.) Terms are as defined in Eq. 2 and Eq. 4b, with slope=d and offset=c. % explained corresponds to that part of  $\sigma^0_{J2-J1}$  explained by the model of Eq. 4b.